A design strategy developed for long term stability of porous PEEK implants through the combined regulation of porous structure and in vivo mechanical stimulation

Yingjie Liu[1,2], Ling Wang[1,2*], Jie Zhang[3,4], Shuguang Liu[3], Jibao Zheng[1,2], Jianfeng Kang[5], Enchun Dong[1,2], Changning Sun[1,2], Ruhan A[6], Chaozong Liu[7], Chuncheng Yang[8], Dichen Li[1,2*]

[1] State Key Laboratory for Manufacturing System Engineering, School of Mechanical Engineering, Xi'an Jiaotong University, Xi'an, Shaanxi, China

[2] National Medical Products Administration (NMPA) Key Laboratory for Research and Evaluation of Additive Manufacturing Medical Devices, Xi'an Jiaotong University, 710054, Xi'an, ShaanXi, China

[3] Academy of Orthopedics, Guangdong Province, Orthopaedic Hospital of Guangdong Province, The Third Affiliated Hospital of Southern Medical University, Guangzhou, China

[4] Department of Oral and Maxillofacial Surgery, Center of Stomatology, Xiangya Hospital, Central South University, Changsha, Hunan, China

[5] School of Mechatronic Engineering and Automation, Foshan University, Foshan, 528225, China

[6] Center for Medical Device Evaluation of NMPA, Beijing, China

[7] Institute of Orthopaedic & Musculoskeletal, University College London, Royal National Orthopaedic Hospital, Stanmore, UK

[8] Shaanxi Jukang Gobo Medical Technology Co.,Ltd., Xi'an, Shaanxi, China

***Corresponding authors:**

Ling Wang

Email: menlwang@xjtu.edu.cn

Address: State Key Laboratory for Manufacturing Systems Engineering Xi'an Jiaotong University, Xi'an 710054, Shaanxi, China

Dichen Li

Email: dcli@xjtu.edu.cn

Address: State Key Laboratory for Manufacturing Systems Engineering Xi'an Jiaotong University, Xi'an 710054, Shaanxi, China

Preprint of Bio-Design and Manufacturing (unedited)

Highlights

[1] The combined influence of porous structure and in vivo mechanical stimulation on the osseointegration performance of PEEK implant was investigated.

[2] The 3D printed porous PEEK prostheses with the optimized pore size achieved good osseointegration in clinical applications.

[3] The active regulation of the mechanical environment that bone experiences in vivo after implantation can be achieved by screw preload.

[4] New bone growth after implantation agrees with the numerical simulations.

[5] Porous PEEK prostheses demonstrated better clinical performance than solid PEEK prostheses.

Abstract

The bioinert nature of PEEK material limits the widespread clinical application of PEEK implants. Although the porous structure is believed to improve the osseointegration performance of PEEK implants, it is hardly used due to the decreased mechanical properties. This study investigates the combined influence of the porous structure and the in vivo mechanical stimulation on implantation safety and bone growth based on the finite element analysis of the biomechanical behavior of the implantation system. It is shown that with the combined control of pore size and screw preloads, the porous PEEK implant can achieve good osseointegration while maintain a relatively high safety level. The optimal combination of pore size and the screw preload are derived. With the pore size of 600 μm and the preload of 0.05 N·m, the safety factor of the implant exceeds 2, and the predicted percentage of the effective bone growth area of the bone-implant interface reaches 97%. The PEEK implants were fabricated by FFF 3D printing technique for further clinical applications. The clinical outcomes demonstrated the better bone repair efficacy and long-term stability of the porous PEEK implants compared to the solid PEEK implants. Good osteointegration performance of the 3D printed porous PEEK implants was shown with the average BV/TV exceeding 40% 3 months after implantation. In conclusion, the 3D printed porous PEEK implants have great potential for clinical application with validated implantation safety and good osseointegration.

Preprint of Bio-Design and Manufacturing (unedited)

Graphic abstract

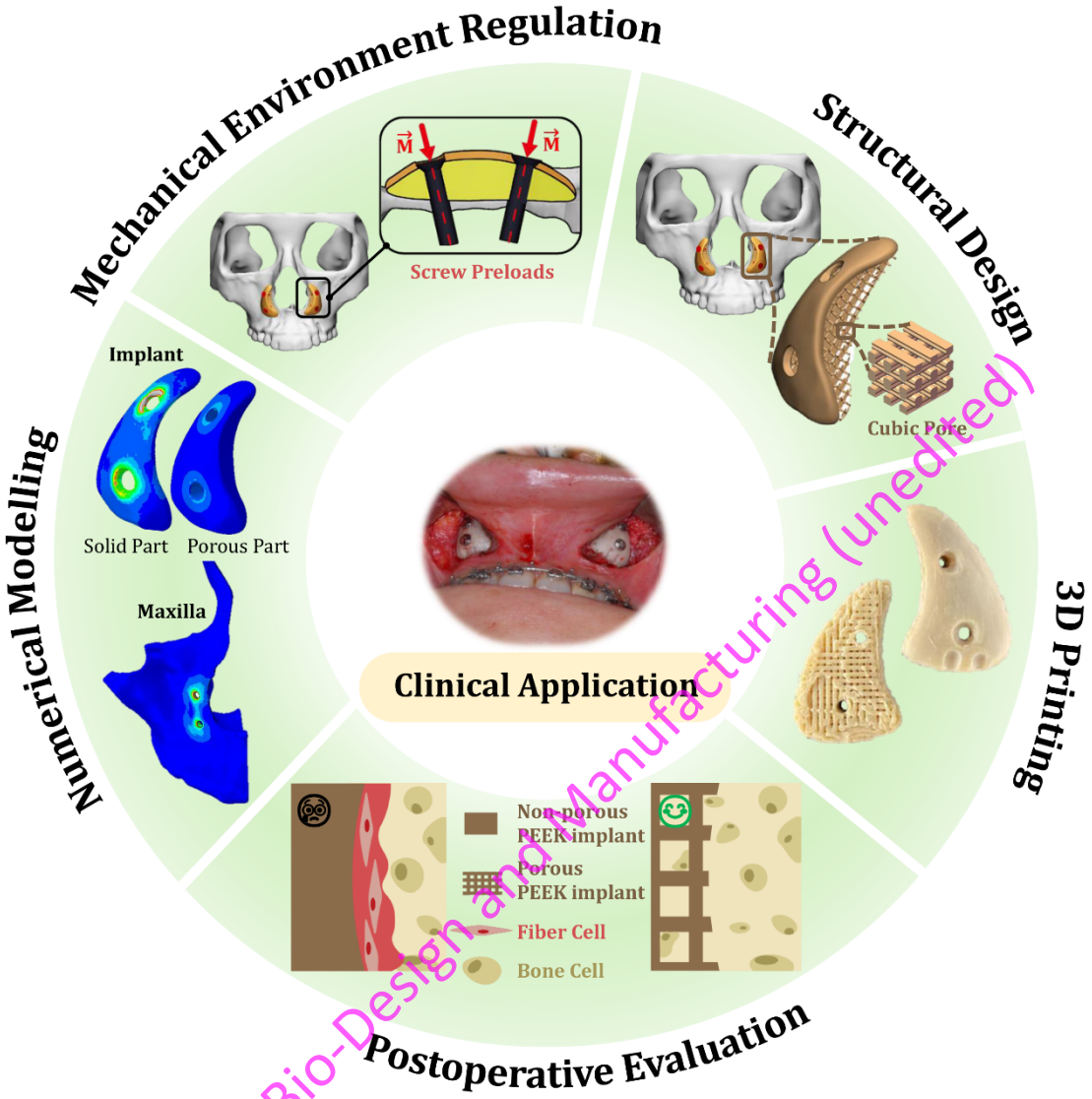

Preprint of Bio-Design and Manufacturing (unedited)

Keywords

Porous PEEK implant, osteointegration, interface biomechanics, maxillofacial implants, Finite Element Analyses, FFF 3D printing

1. Introduction

Polyether ether ketone (PEEK), as an ideal material for bone tissue repair, has been widely utilized in orthopedic and dental fields, with the potential to replace titanium alloys[1]. In recent years, 3D printed PEEK implants have garnered increasing clinical applications due to their ability to match the geometric features and mechanical properties of patients' anatomy[2]. Among these applications, the use of 3D printed PEEK implants in the reconstruction of maxillofacial bone has received particular attention[3], because the bone autografts, as the gold standard, usually cannot recapitulate the maxillofacial contours appropriately and aesthetically and have an unpredictable resorption rate[4].

Despite its potential benefit, the further application of 3D printed PEEK implants is hindered by the bioinert nature of PEEK material itself, which is associated with poor osseointegration post-implantation[5]. Various strategies have been explored to improve the osseointegration of PEEK implants, including composite formation, surface modification, drug loading and porous structure construction[6]. However, except for the construction of porous structure, all other methods lead to property changes of PEEK material itself, which creates additional difficulties for the wide range clinical applications, as the long-term effects of the property changes on the human body need to be evaluated and proven first[7].

The porous structure of PEEK implants can be fabricated by traditional methods such as porogen templating, gas foaming and sulfonation and the 3D printing techniques including fused filament fabrication (FFF) and selective laser sintering (SLS). Porogen templating[8] and gas foaming[9] can produce porous PEEK structures with pore sizes ranging from tens to hundreds of microns while sulfonation[10] can produce nanometer-sized pore structures, all of which were shown to be beneficial for osseointegration. However, the traditional methods are lack of precise control of the pore sizes, architecture and distribution to meet the individual requirements for bone defect repair in various areas. Thus, the 3D printing techniques have been gradually replacing the traditional methods. Zheng[11] prepared PEEK composite scaffolds by FFF printing with tunable elastic modulus in the range of 50.6 to 624.7 MPa by changing pore sizes from 200 to 2000 μm. Wang[12] fabricated PEEK scaffolds by SLS printing with elastic modulus ranging from 42.17 to 512.12 MPa by controlling volume fractions from 20% to 40%. Both of them were similar to the variation range of natural cancellous bone[13]. Similarly, Gummadi[14], Du[15], Spece[16] and Jia[17] et. al. have achieved highly controllable mechanical properties of PEEK scaffolds by controlling the pore sizes, porosity, pore architecture and pore distribution, respectively. In addition to mechanical properties, Feng[18]

Preprint of Bio-Design and Manufacturing (unedited)

investigated the influence of pore size on the osseointegration performance, and cell adhesion and bone formation of 3D printed porous PEEK scaffold were validated by both in vitro cell culture and in vivo animal implantation studies[11,17,19].

In summary, existing literature about the design of porous PEEK structures generally focuses on an isolated aspect rather than combined mechanisms. The influence of porous structures on the mechanical property and bone growth was investigated separately, despite the fact that the changes in the mechanical property of the implant can affect the stress distribution of the surrounding bone tissue and further lead to changes in bone growth[20]. Meanwhile, a majority of in vivo animal studies of porous PEEK scaffolds were conducted in regions bearing low stress and the effect of in vivo mechanical loads on osseointegration was often ignored. However, in actual clinical applications, the mechanical loads are a crucial consideration in the prosthetic design process. On one hand, the porous structure may to some extent compromise the safety of the implant, and on the other hand, variations in mechanical stimuli can influence bone growth. There is limited research on porous PEEK implants targeting clinical applications, and the combined influence of porous structure and in vivo mechanical loads on the implantation safety and osseointegration performance of porous PEEK implants has not been adequately studied. Moreover, to date, there have been no reported clinical applications of 3D printed porous PEEK implants.

This study takes the paranasal implants as the research object, aiming to investigate the combined influence of the pore structure and the in vivo mechanical stimuli on the implantation safety and osseointegration based on the finite element (FE) analysis of the biomechanical behavior of the implantation system. The clinical applications of the 3D printed PEEK implants for paranasal augmentation were then carried out to further validate the clinical efficacy of the porous PEEK structure.

Preprint of Bio-Design and Manufacturing (unedited)

2. Materials & Methods

2.1. Materials & Equipment

The raw material used for manufacturing the prosthesis and scaffold in this study is biological grade PEEK powder (150PF, Victrex Plc, Lancashire, UK). The powder was fed into a twin-screw extruder and extruded into filaments with a diameter of 1.75 mm, which were then printed using an FFF 3D printer (Surgeon Plus, Jukang Gobo Medical Technology, Shaanxi, China). The printing parameters used in this study were as follows: nozzle diameter of 0.4 mm, nozzle temperature of 420°C, printing speed of 20 mm/s, and layer height of 0.2 mm.

2.2. Compressive test for porous PEEK sample

To investigate the variation in mechanical properties of porous PEEK structures with different pore sizes, this study prepared cubic pore PEEK scaffold specimens with pore sizes of 0, 200, 400, 600, 800, and 1000 μm (N=6, length, width, and thickness of 10 mm each) for compression testing to obtain the equivalent mechanical properties of porous PEEK structures with different pore sizes. The uniaxial compression tests were conducted using a universal mechanical testing machine (CMT4304, MTS Corp, USA) at a compression speed of 3 mm/min[11], and the compression direction was along the vertical printing direction of the scaffolds. The force-displacement curves during the compression of the porous structures were recorded and converted into stress-strain curves based on the dimensional characteristics of the porous structures. The elastic modulus was calculated based on the slope of the initial linear stage of the stress-strain curve. The yield strength was calculated when there was a measurable change in the slope.

2.3. Biomechanical studies of porous PEEK implant and interfacial bone

(1) Design of porous PEEK implants for paranasal augmentation

Paranasal defects are a common type of midfacial deformity caused by maxillofacial trauma or developmental abnormalities of the maxilla[21,22]. The clinical data for this study were sourced from the third affiliated hospital of Southern Medical University (Guangzhou, China). Patients underwent CT scans for head, and the CT images were used to construct models of maxillofacial bones in MIMICS software (Version 20.0, Materialise, Inc., Leuven, Belgium) for assessing paranasal defects and the geometric design of the implants, as shown in Fig. 1(a-b). Based on anatomical consistency as the design criterion[23], implant models were established on both sides of the paranasal area and a smooth transition between the implant and the maxillary bone was achieved. The outer region in contact with the soft tissue was designed as solid with a thickness of about 1 mm to prevent soft tissue from invading into the porous structure. This part of the PEEK implant will be referred to as the 'solid part' in the following text. The bottom region of the implant in contact with the host bone was designed as uniform cubic porous structures. This part of the PEEK implant will be referred to as the 'porous part' in the following text. When the pore size of the porous part becomes zero, the entire PEEK implant turns to be solid. To prevent rotation of the implant, bilateral anchoring screws were used for fixation, with a diameter of 2 mm, a length of 10 mm, and a pitch of 0.4 mm, supplied by Waston Medical (Changzhou, China).

Preprint of Bio-Design and Manufacturing (unedited)

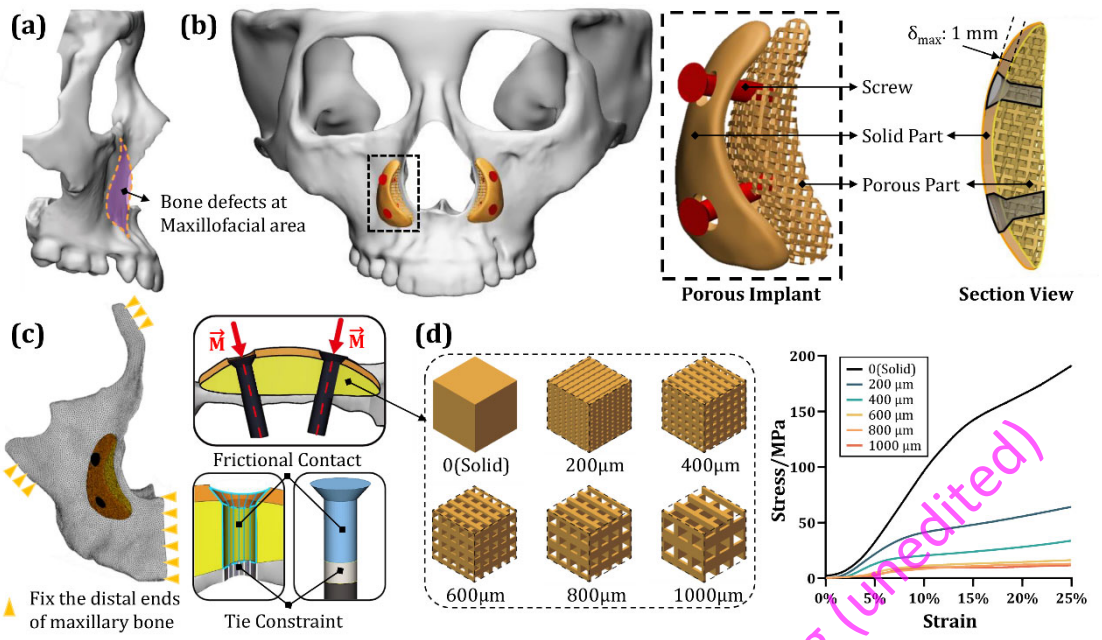

Fig. 1 3D model of the maxillofacial bone and porous PEEK implants and FE model setup for this study. (a) The reconstructed maxillofacial bone with paranasal defects. (b) The porous PEEK implants for paranasal augmentation. Each PEEK implant consisted of the solid part and the porous part and was fixed on the maxillofacial bone by two screws. (c) Boundary conditions, contacts and interactions of the FE model. (d) Schematic diagram of the 3D unit cells of the porous PEEK structures with different pore sizes and the representative stress-strain curves of them, which could be divided into three stages: elastic, plateau and densification.

Preprint of Bio-Design and Manufacturing (unedited)

(2) FE model of the PEEK implant, the maxillofacial bone and screws

A numerical model of the bone in the paranasal area and the prosthesis was established and analyzed using the FE method in ABAQUS software (Version 6.14, Abaqus Inc., USA). As shown in Fig.1c, the FEM model in this study includes three parts: the unilateral maxillary bone, the implant, and two screws. Table 1 lists the mechanical properties of each part, assuming that all materials are homogeneous, isotropic, and linearly elastic. The PEEK implant consists of both the solid part and the porous part, as described in 2.3. To save computational costs, the equivalent material properties of the porous PEEK structures obtained from the compression tests described in section 2.2 were used for the porous part of the PEEK, with the feasibility confirmed in the previous studies[24,25]. The model was meshed with quadratic 10-node tetrahedral elements (C3D10), and a sensitivity analysis was conducted until a change of <5% in the maximum Von Mises stress was obtained by mesh refinement. Finally, a mesh size of 0.25 mm was set.

Table 1 Mechanical properties of the materials used in FEM model

Components	Porous (μm)	Elastic modulus (MPa)	Poisson's ratio	Yield strength (MPa)	Ref
PEEK	0	1305	0.3	148	\
	200	551	0.3	41	
	400	414	0.3	23	
	600	190	0.3	12	
	800	150	0.3	11	
	1000	127	0.3	10	
Maxillary bone	\	12000	0.3	88	[26]
Titanium screws	\	110000	0.3	850	[26]

The boundary conditions and loads on the model were set according to the mechanical environment of the prosthesis in the human body. The paranasal region of the maxillary bone bears relatively low stress (less than 1MPa) under normal physiological conditions[27,28] and the tightening loads on the screws were considered as the major loads. The area where the maxillary bone connects with adjacent bones was set to be fully constrained. Bonding constraints were applied to the interface between the screws and the maxillary bone to ensure that there is no relative displacement between the screws and the host bone. The "Bolt Load" feature in ABAQUS was used to apply tightening forces to the two screws, with the input force being converted into tightening torque using the following formula:

$$F = 1000M / K \cdot d \tag{1}$$

In the formula, F represents the tightening force in Newtons (N); M is the tightening torque in Newton-meters (N·m); K is the torsional coefficient (0.3); d is the nominal diameter of the thread, which is set to be 2 mm. The tightening load of the two screws is kept consistent with each other for all models.

(3) Parameterized study of implantation safety and bone growth

The in vivo mechanical performance and stress distribution of each component of the implantation under various pore sizes (0~1000 μm) and screw preloads (0.01~0.09N·m) was investigated. The safety factors of each component were assessed by comparing the ratio of the maximum stress obtained through FE analysis to the yield stress. The strain distribution of the bone-implant interface and the bone-screw interface were extracted to assess the bone growth based on the Wolff's law. The effective bone growth area of the interface was calculated to predict the osseointegration performance of the implant. After evaluating the combined influence of the pore structure and the in vivo mechanical loads, the optimal pore size and

Preprint of Bio-Design and Manufacturing (unedited)

screw preload were selected to achieve both good implantation safety and osseointegration performance for further clinical applications.

2.4. Clinical applications for PEEK implants

Fifteen patients (14 female and 1 male) with an average age of 26±3 years were recruited at the third affiliated hospital of Southern Medical University. This study was reviewed and approved by the hospital, while the 3D printed PEEK implants were approved by State Key Laboratory for Manufacturing Systems Engineering. The Patient selection and inclusion criteria were described in detail in our previous study[29]. The study was performed by the Declaration of Helsinki's ethical principles and international norms and was approved by the Ethics Committee of the Hospital (EC-CT-[2019]28). All subjects signed a written informed consent before their inclusion in the study. Patients were randomly assigned to two different groups. One group (7 patients) received treatment with 3D printed solid PEEK implants and the other group (8 patients) received treatment with 3D printed porous PEEK implants with the optimal pore size obtained in 2.3.

All the patients underwent surgery in the third affiliated hospital of Southern Medical University. Patients were followed up at 3 days, 3 months, and 6 months postoperatively, and a CT scan of the head was performed each time. The average Hounsfield unit (HU) values of the bone-implant interface and the PEEK prostheses were calculated based on the CT scans. The maxillofacial bone, PEEK prostheses and the newly formed bone tissue were three-dimensional reconstructed. The bone volume fraction (BV/TV) was obtained, which represented the ratio of the newly formed bone volume to the pore volume of the prosthesis and could directly reflect the changes in the newly formed bone volume.

2.5 Statistical analyses methods

Experimental data were presented as mean ± standard deviation. Statistical analyses were performed using GraphPad Prism 9.0 software (GraphPad Software, USA) or Origin 2024 software (Origin Software, USA). Data were analyzed using one-way analysis of variance (one-way ANOVA) and Tukey's multiple comparison test. The criteria for significant differences were $P<0.05$ (*) and $P<0.01$ (**).

3 Results

3.1. The stress distribution on the implants

The biomechanical behavior of the PEEK implant, maxillary bone and the screws were analyzed based on the FE method. The influence of various pore structures and preloads were mainly on the stress values of each component and there was little difference in the stress

Preprint of Bio-Design and Manufacturing (unedited)

distribution. The representative stress distribution of each component with pore size of 600 μm and preload of 0.05 N·m are shown in Fig. 2. The results indicated that the von Mises stress in the maxillary bone was mainly distributed at the bone-implant interface, with the maximum stress occurring at the edge of the screw hole. The farther away from the screw holes, the lower the von Mises stress value. And the average value of the stress in the region between the two screws was one-fifth of the maximum stress. For the PEEK implant, the stress was also concentrated around the screw holes and the maximum stress in the solid part was 6 times higher than in the porous part.

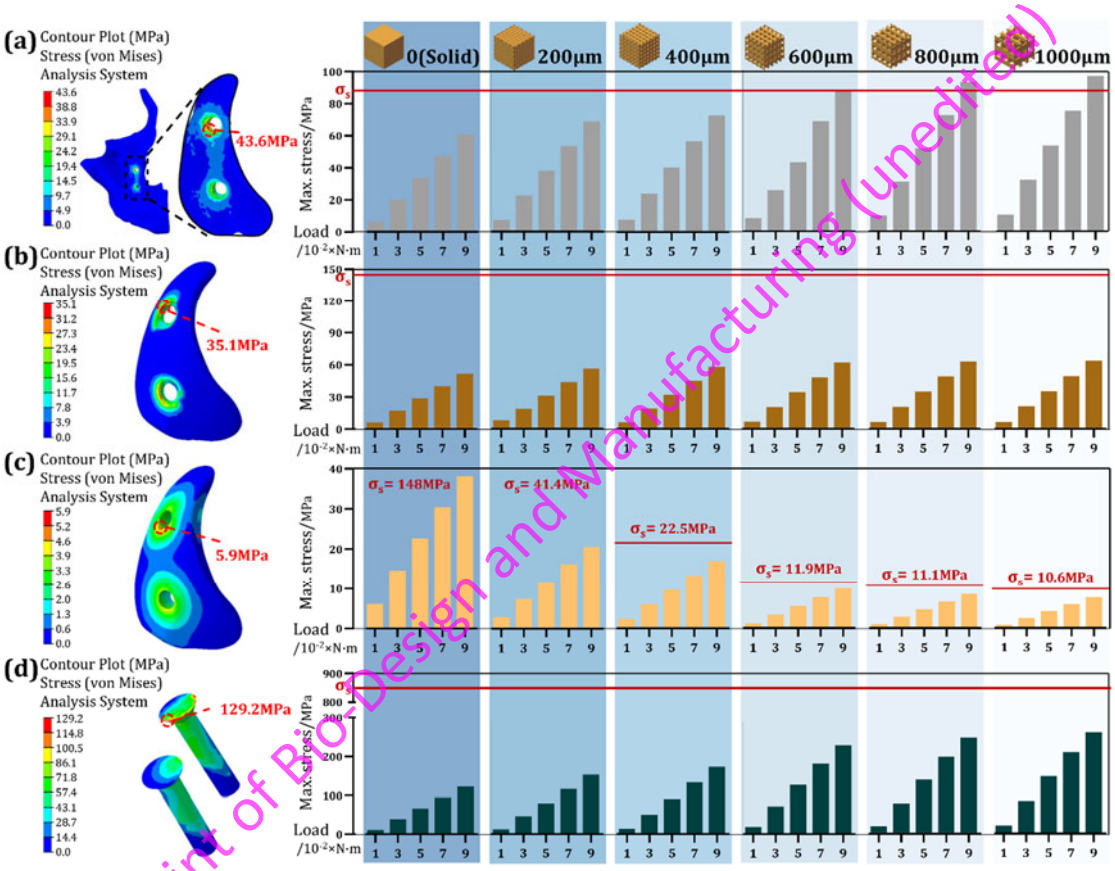

Fig. 2 The representative Von Mises stress distribution and the predicted maximum von Mises stress at various pore sizes and preloads of (a) the maxillary bone with the zoomed-in area of interfacial bone, (b) the solid part of PEEK implant, (c) the porous part of PEEK implant and (d) the screws. The representative von Mises stress distribution is under pore size of 600 μm and preload of 0.05 N·m. The yield strength of each component is marked with a red line. For the porous part of PEEK implant, the yield strength changed with the various pore sizes.

Preprint of Bio-Design and Manufacturing (unedited)

3.2. Safety analyses

The variation of the maximum von Mises stress of each component under the combined influence of pore sizes and preloads is shown in Fig. 2. The maximum stress of each component increased noticeably with the increasing preload at different pore sizes and the amount of

increase was proportional to the stress value of the component itself. The maximum stress of the maxillary bone and the screws increased as the pore size increased. The increase of the maximum stress of the solid part of the PEEK implant was not obvious while an obvious decrease was shown of the maximum stress of the porous part of the PEEK implant with the increasing pore size. The maximum stress on the maxillary bone exceeded its yield strength when the preload was greater than 0.09 N·m and the pore size was greater than 600 μm, which means the bone fracture might happen after implantation.

The variation of the safety factor of each component under the combined influence of pore sizes and preloads was further analyzed, as shown in Fig. 3. The safety factor of the screws was significantly higher than those of the other components. It is shown that the influence of the preload on the safety factor was more obvious. And when the preload increased, the influence of the pore size on the safety factor diminished. When the preload exceeded 0.07 N·m, the safety factor of the PEEK implant and the maxillary bone dropped below 2 at all pore sizes. For the porous part of the implant, the increase in pore size led to a decrease in the maximum stress and in the yield strength at the same time, which ultimately resulted in a decrease of the safety factor. And the influence of the pore size on the porous part of the implant was the most obvious among all the components. Taken together, smaller pore size and lower preload were more beneficial to the implantation safety of all components.

Preprint of Bio-Design and Manufacturing (unedited)

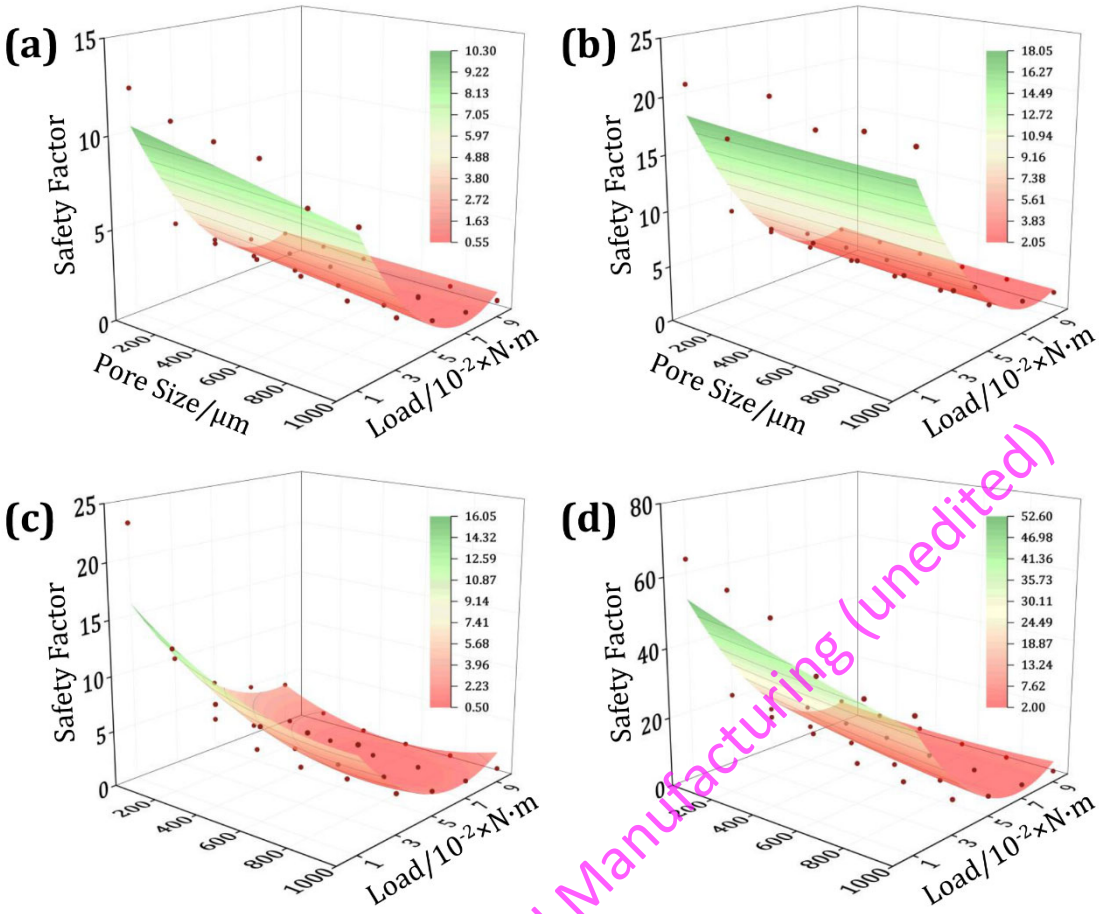

Fig. 3 The combined influence of the pore size and preload on the safety factor of (a) the maxillary bone, (b) the solid part of PEEK implant, (c) the porous part of PEEK implant and (d) the screws.

Preprint of Bio-Design and Manufacturing (unedited)

3.3. The strain distribution of the interfacial bone and bone growth analyses

The strain distribution of the bone-implant interface and the bone-screw interface under different pore sizes and preloads was investigated, as shown in Fig. 4. The average strain at the bone-screw interface is higher than that at the bone-implant interface under the same conditions, and the maximum strain at the bone-implant interface primarily concentrates around the two screw holes. The bone growth of the interfacial bone was further predicted by the Wolff's law with the effective bone growth area defined as the area of where the strain was in the range of 50 to 3000 με. The bone growth of the bone-implant interface was related to the osseointegration performance of the PEEK implant, while the bone growth of the bone-screw interface was related to the long-term stability of the screw connections[30].

For the bone-implant interface, the increase in pore size markedly increased the effective bone growth area when the preload was low. When the preload was only 0.01 N·m, the effective bone growth area with pore size of 600 μm was three times larger than that with pore size of

0 (solid implant). The increase in preload also increased the effective bone growth area. When the pore size was 0 (solid implant), the preload needed to be increased to above 0.07 N·m to keep the majority of the bone-implant interface within the effective bone growth range. However, when the preload and the pore size exceeded a certain level, the strain at the bone-implant interface near the screw holes became larger than 3000 με, which led to a reduction in the effective bone growth area. For the bone-screw interface, the entire interface was within the effective bone growth range under the minimum pore size (0) and preload (0.01 N·m). And as the pore size and preload increased, the effective bone growth area decreased continuously with the strain in the peripheral area of the interface exceeding 3000 με.

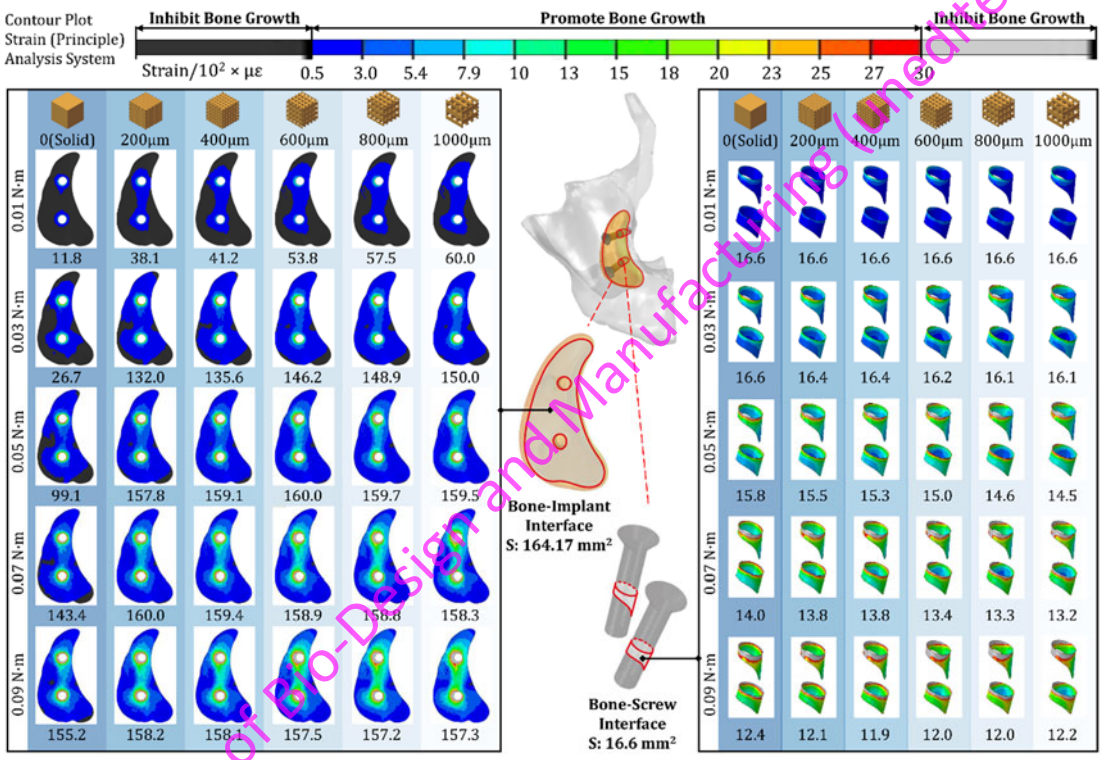

Fig. 4 The predicted strain distribution and effective bone growth area of the bone-implant interface and the bone-screw interface with various pore sizes and preloads. The data under each strain distribution diagram is the effective bone growth area in mm².

The percentage of the effective bone growth area in the bone-implant interface and the bone-screw interface were calculated, as shown in Fig. 5. The result shows that the percentage in the bone-implant interface reached it maximum 97.4% when the pore size was 600 μm and the preload was 0.05 N·m or when the pore size was 200 μm and the preload was 0.07 N·m, as marked by the yellow asterisks in Fig. 5. However, the percentage in the bone-screw interface with the pore size of 600 μm and the preload of 0.05 N·m (90.2%) was higher than that with the pore size of 200 μm and the preload of 0.07 N·m (83.0%), which was beneficial to the screw

Preprint of Bio-Design and Manufacturing (unedited)

fixation and the long-term stability of the implant. Considering the combined influence of the pore size and preload on the implantation safety and the osseointegration performance, the pore size of 600 μm and the preload of 0.05 N·m was chosen as the optimal combination to improve bone growth while maintain safety. With the optimal combination, the safety factor of each component exceeded 2 and the percentage of the effective bone growth area in the bone-implant interface was 97.4%.

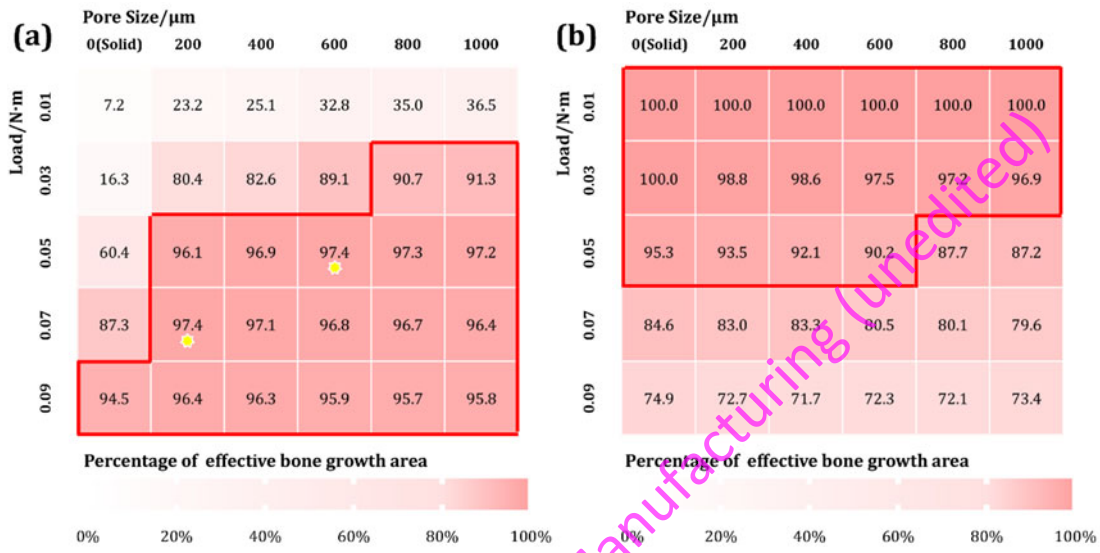

Fig. 5 The percentage of the effective bone growth area under various pore sizes and preloads (a) of the bone-implant interface and (b) the bone-screw interface. The combinations of the pore size and the preload that resulted in a percentage higher than 90% were framed by the red line. The combinations of the pore size and the preload that resulted in the highest percentage were marked by a yellow asterisk.

Preprint of Bio-Design and Manufacturing (unedited)

3.4. Clinical outcomes

A total of 15 clinical applications have been carried out, including the solid PEEK implant group (7 patients) and the porous PEEK implant group (8 patients). The average thickness of the PEEK implants was 5±1.5 mm fabricated using FFF 3D printing technology. The uniform cubic pore structure design with pore size of 600 μm was used for the porous PEEK implants, as shown in Fig. 6a. Different preloads on the screws were applied to the two groups in the surgery, with 0.07 N·m preloads to the solid PEEK implant group and 0.05 N·m preloads to the porous PEEK implant group, according to the results in 3.3. During the surgical procedure, all implants in both groups perfectly matched the geometric shape of the defect maxillary bone, and no implant migration, extrusion, or rupture occurred post-surgery.

The representative postoperative CT images of the solid PEEK implant group and the porous PEEK implant group are shown in Fig. 6b-d. The characteristic of the porous structure of the

porous PEEK implant was seen clearly on the CT at 3 days after surgery (Fig. 6b) as marked by the blue arrows, while no radiolucent area of the porous structure was seen at the same region on the CT at 3 months after surgery (Fig. 6c), indicating the new bone formation within the porous structure of the porous PEEK implant. However, the bone growth and osteointegration performance of the solid PEEK implant was not ideal as s gap between the solid implant and the maxillary bone was seen on the CT at 3 months after surgery (Fig. 6d).

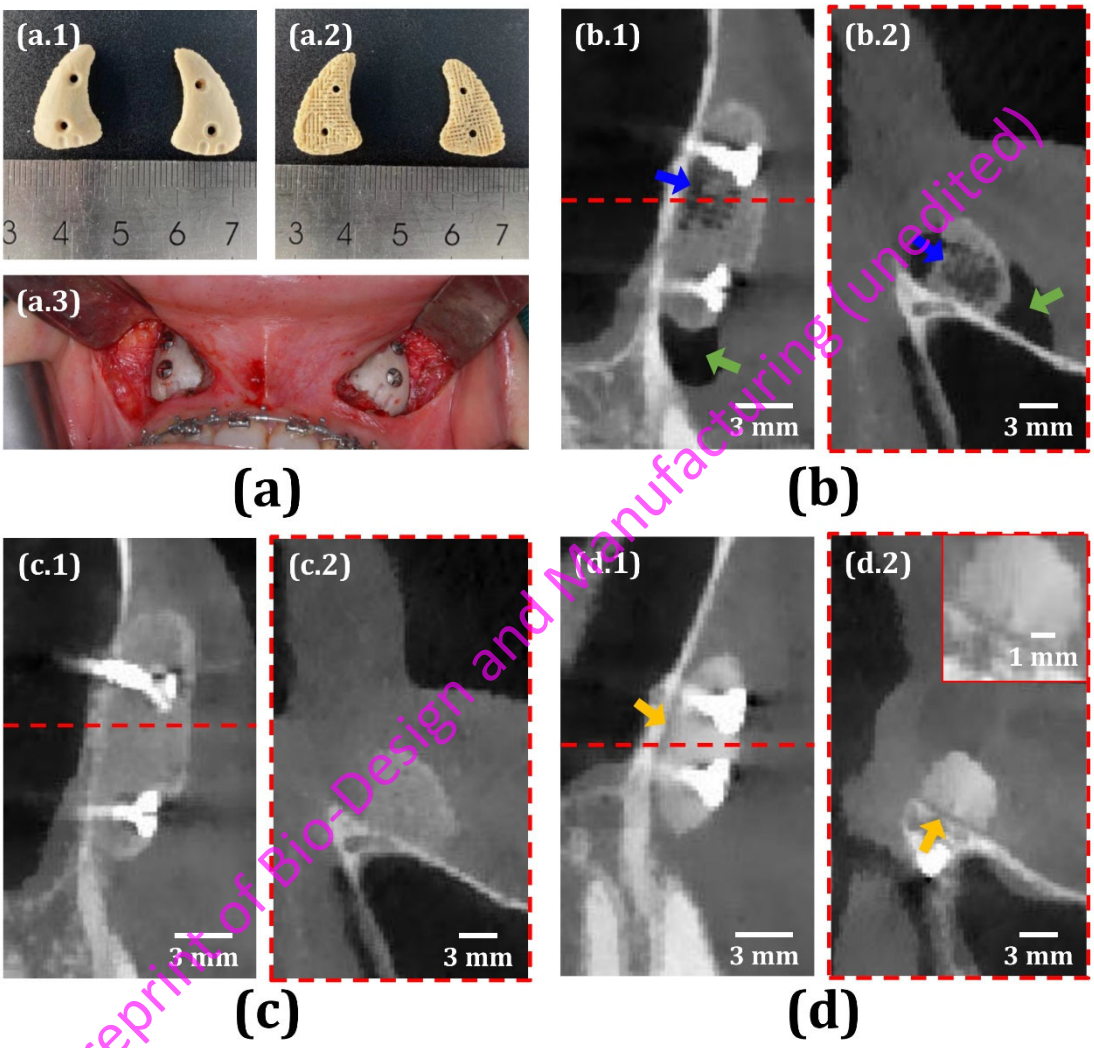

Preprint of Bio-Design and Manufacturing (unedited)

Fig. 6 The representative intraoperative photos and postoperative CT images. (a) Front (a.1) and backside (a.2) of the 3D printed porous PEEK implants; (a.3) PEEK prostheses after implantation; (b) CT images of the 3D printed porous PEEK implant at 3 days post-operative (b.1) in coronal plane, (b.2) in sagittal plane, blue arrow indicates porous structure, green arrow points to the incisions; (c) CT images of the 3D printed porous PEEK implant at 3 months post-operative (c.1) in coronal plane, (c.2) in sagittal plane; (d) CT images of the 3D printed solid PEEK implant at 3 months post-operative (d.1) in coronal plane, (d.2) in sagittal plane, yellow arrow points to the gap between the bone and implant.

Based on the CT images, the 3D models of the PEEK implants and the new bone within the implants of the porous PEEK implant group 3-month after surgery were reconstructed, as shown in Fig. 7a. It is shown that the new bone formation was mainly concentrated in the central area of the implants, especially around the screw holes, which was consistent with the effective bone growth region results obtained in 3.3, Fig. 4. The average BV/TV of the porous part of the porous PEEK implants of the porous PEEK implant group was calculated and reached 42.2% 3 months after implantation and 59.9% 6 months after implantation. A significant increment of HU value of the porous part of the porous PEEK implants was seen, also indicating the increasing new bone formation within the porous PEEK implants (Fig. 7c).

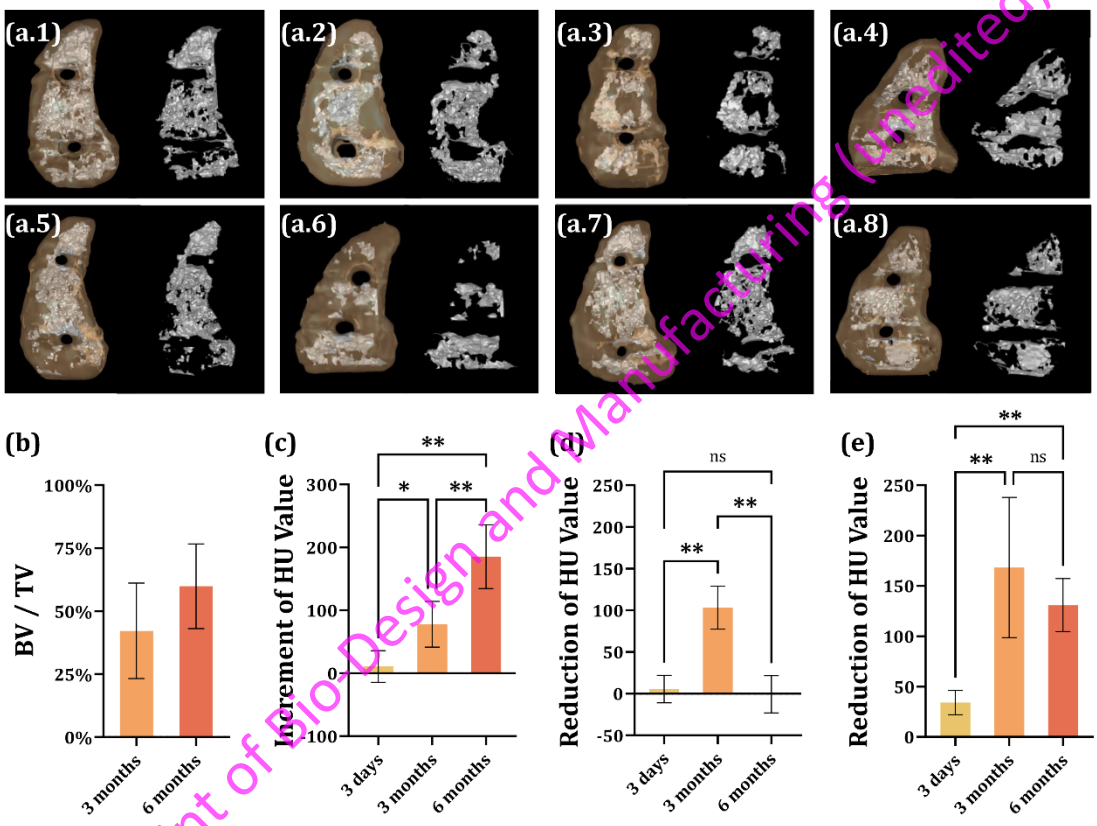

Preprint of Bio-Design and Manufacturing (unedited)

Fig. 7 The analysis of bone growth after implantation. (a) The reconstructed 3D models of PEEK implants with new bone (left) and new bone extracted separately (right) based on the CT images 3 months after surgery. (a.1)~(a.8) refers to eight different patients in the porous PEEK implant group. (b) BV/TV of the porous implants 3 months and 6 months after implantation. (c) The increment of HU value of the porous part of the porous PEEK implants in the porous PEEK implant group at different time points after surgery. (d) The reduction of HU value of the bone-implant interface of the patients in the porous PEEK implant group at different time points after surgery. (e) The reduction of HU value of the bone-implant interface of the patients in the solid PEEK implant group at different time points after surgery. The baseline HU value of the comparison in (c)~(e) is the initial HU value of the relevant object

shortly before implantation. The criteria for significant differences were P<0.05 (*) and P<0.01 (**).

To further compare the bone growth at the bone-implant interface between the porous PEEK implant group and the solid PEEK implant group, the change of HU value at the interface was calculated, as shown in Fig. 7d and 7e. The HU value at the interface of the patients in the porous PEEK implant group decreased at 3 months postoperatively but returned to preoperative values at 6 months postoperatively (Fig. 7d), suggesting a good bone growth status. However, the HU value at the interface of the patients in the solid PEEK implant group significantly decreased at both 3/6 months postoperatively (Fig. 7e). In conclusion, it is evident that osseointegration performance of the 3D printed porous PEEK implants was better than that of the 3D printed solid PEEK implants based on the comparison of CT images and the change of HU value between the two groups.

4. Discussion

Although the PEEK implants have been widely used, most of them are solid without porous structures. There are only a few reports[31,32] on the clinical application of the porous PEEK implants and none of them were manufactured via 3D printing. A classic example of the clinically used porous PEEK implants is the PEEK Interbody Fusion Cage (COHERE@)[32], where the pores were created by porogen templating, in which enhanced bone bonding and spinal fusion occurred. However, the porous structure of the PEEK Interbody Fusion Cage does not allow the free design in terms of pore architecture, pore size or pore distribution, which play an important role in osseointegration. There are few studies focusing on the design of the porous structure of PEEK prostheses. Moiduddin[33] analyzed the stress distribution and the deformation of a cranial PEEK implant with a uniform diamond pore structure with a 1350 pore size and 70% porosity under physiological load by FE method. Sharma[31] compared the mechanical behaviors of the PEEK orbital mesh implants with three different porous constructs. Although implantation safety was considered in these studies, the influence of the porous structure on bone growth and osseointegration performance was not mentioned. In this study, the structural design of the porous PEEK implants is investigated together with the in vivo mechanical stimulation to achieve good implantation safety and osseointegration simultaneously and is validated with good clinical outcomes.

Despite the potential for better osseointegration, the wider application of porous PEEK implants is hindered by the major concern of the decrease in the mechanical properties with the construction of porous structures. The elastic modulus and the yield strength of the solid

Preprint of Bio-Design and Manufacturing (unedited)

PEEK structure (E=1305 MPa; σ_s=148 MPa) are close to that of the cancellous bone (E=20-500 MPa; σ_s=4-12 MPa) and lower than that of the cortical bone (E=3000-30000 MPa; σ_s=130-180 MPa)[13]. For the solid PEEK prostheses used in bone reconstruction in the high load-bearing area, such as hip implants[34], rib prostheses[35] and mandibular implants[26], the safety factor was already at 2-3 according to the previous research. Considering the lower mechanical properties of the porous PEEK structure (E=127-551 MPa; σ_s=10-41 MPa), the application of the porous PEEK prostheses in the high load-bearing area required further and careful considerations about safety and stability. Relatively speaking, the porous PEEK prostheses are more suitable for reconstruction in the low load-bearing area, such as maxillofacial bone. Therefore, the paranasal defect was selected for this study with screw preloads applied as major loads. It was shown that the porous PEEK protheses became more sensitive to the loads when the pore size increased, with a noticeable decrease in safety factor caused by a slight increase in preload, emphasizing the importance of taking into consideration of the loading environment characteristics during the porous designing procedure.

In addition to the mechanical safety, consideration related to bone growth and osseointegration is another key factor for the design of the porous structure of PEEK implant. This study investigated the influence of the pore size on bone growth based on Wolff's law and improved the osteointegration performance of the porous PEEK implant by mechanical environment regulation. According to previous research, pore size also affects bone growth by affecting osteocyte behavior and nutrient transport[36]. And the pore size of 600 μm was found to achieve high fixation ability and deep bone ingrowth in the early period[37], improve osteoinduction[38] and neovascularisation[39]. Therefore, the pore size of 600 μm was ultimately selected in this study while the alternative pore size could also achieve a high percentage of effective bone growth area of the bone-implant interface with appropriate preloads. Besides the pore size, other design parameters of the porous structure, such as the pore architecture[40] and the pore distribution[41], also affect bone growth.

The mechanical environment of the implant-bone interface was adjusted in a controlled manner by the combined control of both pore structure and preload in this study, with optimized purposes of bone growth rate at the interface. The active regulation of the in vivo mechanical stimulation has important clinical significance for the situation where the normal physiological load is not enough for the mechanical stimulation for bone growth after implantation, similar to the effect of the stress shielding associated with metal implants. The active regulation of the in vivo mechanical stimulation was achieved by the application of

Preprint of Bio-Design and Manufacturing (unedited)

screw preloads in this study to improve the interfacial bone growth. The stability of the screw connection needs to be concerned in the regulation of the screw preloads. As shown in 3.3, the changing trends of the effective bone growth area at the bone-implant interface and at the bone-screw interface were inconsistent and a trade-off has to be made.

Good clinical outcomes and osseointegration performance of the 3D printed porous PEEK implants were achieved with the optimized design, and high consistency was found for those promoted/inhibited bone growth areas between the FE analysis and those clinical data. Based on the CT images, the bone growth at the bone-implant interface of the patients using 3D printed solid PEEK implants was not ideal, though greater preloads were applied according to the FE analysis. This could not benefit long-term bone regeneration and may further lead to osteoporosis. The unsatisfactory bone repair efficacy of the 3D printed solid PEEK implants may be caused by the bioinert nature of PEEK material, which makes it difficult for bone cells to attach and hinders further bone tissue growth. Compared to the solid PEEK implants, the interconnected porous structure of the porous PEEK implants mimicked the extracellular matrix of the native bone tissues and provided space for bone ingrowth, with BV/TV reaching 42.2% 3 months after implantation and 59.9% 6 months after implantation. The integration between the porous structure and new bone improved the interfacial mechanical locking, which contributes to the long-term stability of the implants. Furthermore, the mechanical properties of the PEEK implants can also be improved with the new bone formation, according to the previous study[42]. In summary, the clinical results of this study validated the porous structure benefit for bone growth and osseointegration and highlighted the obvious potential of 3D printed porous PEEK in maxillofacial repair and reconstruction.

Some simplification of the geometry and boundary conditions has been made in the FE model in this study. A more detailed FE model can be built in the future study to investigate the mechanical behavior of the individual cell unit of the porous structure. Different pore architecture and pore distribution, such as the Voronoi-based architecture and the anisotropic pore distribution[43], which have attracted much attention in recent years, can also be considered for the future porous PEEK implant design. Furthermore, the combination of the porous structure design and material modification will be an important development direction for PEEK implants. The PEEK composite with reinforcing fibers can also help to overcome problems associated with weak mechanical properties of the porous PEEK structures[44].

5 Conclusion

Preprint of Bio-Design and Manufacturing (unedited)

Despite the potential advantages in osteointegration, porous PEEK implants are limited in clinical applications due to the safety concern in mechanical stability. In this study, the implantation safety and good osteointegration of porous PEEK implants are achieved by the combined regulation of pore structure and in vivo mechanical stimulation. The clinical applications of the 3D printed porous PEEK implants demonstrated better bone repair efficacy and excellent osseointegration, indicating long-term stability, compared to the solid PEEK implants, validating the clinical feasibility of porous PEEK implants. The strategy for designing the porous PEEK implants in this study lays a foundation for the design and clinical applications of the other types of prostheses in PEEK.

Acknowledgements

The work was supported by National Key R&D Program of China (2023YFB4603500)，the Fundamental Research Funds for the Central Universities and the Program for Innovation Team of Shaanxi Province (2023-CX-TD-17), Shaanxi Province Qinchuangyuan "Scientist + Engineer" Team Construction Project (2022KXJ-106).

Conflicts of interest/Competing interests

We have no financial and personal relationships with other people or organizations that can inappropriately influence our work, there is no professional or other personal interest of any nature or kind in any product, service and/or company that could be construed as influencing the position presented in, or the review of, the manuscript entitled, “Mechanisms investigation on the osseointegration of 3D printed PEEK prostheses: mechanical design to clinical applications”.

Ethics approval

This research has been approved by the Stomatological Hospital, Southern Medical University. The study was performed by the Declaration of Helsinki’s ethical principles and international norms and was approved by the Ethics Committee of the Hospital (EC-CT-[2019]28). All subjects signed a written informed consent before their inclusion in the study.

Author contributions

Yingjie Liu, original draft, design and manufacturing; Ling Wang, original draft, conceptualization; Dichen Li, conceptualization; Jie Zhang and Shuguang Liu, clinical applications; Jibao Zheng , Jianfeng Kang , Enchun Dong, Changning Sun, Ruhan A, Chaozong Liu and Chuncheng Yang, methods;

Reference

Preprint of Bio-Design and Manufacturing (unedited)

[1] Hacherl CC, Patel NA, Jones K, et al (2021) Characterizing Adverse Events of Cranioplasty Implants After Craniectomy: A Retrospective Review of the Federal Manufacturer and User Facility Device Experience Database. Cureus Journal of Medical Science 13 (7): e16795. https://doi.org/10.7759/cureus.16795

[2] Wang L, Yang C, Sun C, et al (2022) Fused Deposition Modeling PEEK Implants for Personalized Surgical Application: From Clinical Need to Biofabrication. International Journal of Bioprinting 8 (4): 615. https://doi.org/10.18063/ijb.v8i4.615

[3] Kauke-Navarro M, Knoedler L, Knoedler S, et al (2024) Surface modification of PEEK implants for craniofacial reconstruction and aesthetic augmentation-fiction or reality? Frontiers in Surgery 11: 1351749. https://doi.org/10.3389/fsurg.2024.1351749

[4] Sakkas A, Wilde F, Heufelder M, et al (2017) Autogenous bone grafts in oral implantology-is it still a "gold standard"? A consecutive review of 279 patients with 456 clinical procedures. International Journal of Implant Dentistry 3: 23. https://doi.org/10.1186/s40729-017-0084-4

[5] Panayotov IV, Orti V, Cuisinier F, et al (2016) Polyetheretherketone (PEEK) for medical applications. Journal of Materials Science-Materials in Medicine 27 (7): 118. https://doi.org/10.1007/s10856-016-5731-4

[6] Zheng Z, Liu P, Zhang X, et al (2022) Strategies to improve bioactive and antibacterial properties of polyetheretherketone (PEEK) for use as orthopedic implants. Materials Today Bio 16: 100402. https://doi.org/10.1016/j.mtbio.2022.100402

[7] Bartelstein MK, Van Citters DW, Weiser MC, et al (2017) Failure of a Polyaryletheretherketone-Cobalt-Chromium Composite Femoral Stem Due to Coating Separation and Subsidence: A Case Report. JBJS case connector 7 (4): e83-e83. https://doi.org/10.2106/jbjs.Cc.16.00280

[8] Evans NT, Torstrick FB, Lee CSD, et al (2015) High-strength, surface-porous polyether-ether-ketone for load-bearing orthopedic implants. Acta Biomaterialia 13: 159-167. https://doi.org/10.1016/j.actbio.2014.11.030

[9] Yang Q, Zhang G, Ma Z, et al (2015) Effects of processing parameters and thermal history on microcellular foaming behaviors of PEEK using supercritical CO₂. Journal of Applied Polymer Science 132 (39): 42576. https://doi.org/10.1002/app.42576

[10] Zhao Y, Wong HM, Wang W, et al (2013) Cytocompatibility, osseointegration, and bioactivity of three-dimensional porous and nanostructured network on polyetheretherketone. Biomaterials 34 (37): 9264-9277. https://doi.org/10.1016/j.biomaterials.2013.08.071

[11] Zheng JB, Zhao HY, Dong EC, et al (2021) Additively-manufactured PEEK/HA porous scaffolds with highly-controllable mechanical properties and excellent biocompatibility. Materials Science and Engineering C-Materials for Biological Applications 128: 112333. https://doi.org/10.1016/j.msec.2021.112333

[12] Wang H, Chen P, Wu H, et al (2022) Comparative evaluation of printability and compression properties of poly-ether-ether-ketone triply periodic minimal surface scaffolds fabricated by laser powder bed fusion. Additive Manufacturing 57: 102961. https://doi.org/10.1016/j.addma.2022.102961

[13] Azami M, Moztarzadeh F, Tahriri M (2010) Preparation, characterization and mechanical properties of controlled porous gelatin/hydroxyapatite nanocomposite through layer solvent casting combined with freeze-drying and lamination techniques. Journal of Porous Materials 17 (3): 313-320. https://doi.org/10.1007/s10934-009-9294-3

Preprint of Bio Design and Manufacturing (unedited)

[14] Gummadi SK, Saini A, Owusu-Danquah JS, et al (2022) Mechanical Properties of 3D-Printed Porous Poly-ether-ether-ketone (PEEK) Orthopedic Scaffolds. Jom 74 (9): 3379-3391. https://doi.org/10.1007/s11837-022-05361-6

[15] Du X, Ronayne S, Lee SS, et al (2023) 3D-Printed PEEK/Silicon Nitride Scaffolds with a Triply Periodic Minimal Surface Structure for Spinal Fusion Implants. ACS Applied Bio Materials 6 (8): 3319-3329. https://doi.org/10.1021/acsabm.3c00383

[16] Spece H, Yu T, Law AW, et al (2020) 3D printed porous PEEK created via fused filament fabrication for osteoconductive orthopaedic surfaces. Journal of the Mechanical Behavior of Biomedical Materials 109: 103850. https://doi.org/https://doi.org/10.1016/j.jmbbm.2020.103850

[17] Jia C-Q, Zhang Z, Cao S-Q, et al (2023) A biomimetic gradient porous cage with a micro-structure for enhancing mechanical properties and accelerating osseointegration in spinal fusion. Bioactive Materials 23: 234-246. https://doi.org/https://doi.org/10.1016/j.bioactmat.2022.11.003

[18] Feng X, Ma L, Liang H, et al (2020) Osteointegration of 3D-Printed Fully Porous Polyetheretherketone Scaffolds with Different Pore Sizes. Acs Omega 5 (41): 26655-26666. https://doi.org/10.1021/acsomega.0c03489

[19] Roskies M, Jordan JO, Fang D, et al (2016) Improving PEEK bioactivity for craniofacial reconstruction using a 3D printed scaffold embedded with mesenchymal stem cells. Journal of Biomaterials Applications 31 (1): 132-139. https://doi.org/10.1177/0885328216638636

[20] Cowin SC, Mosssalentijn L, Moss ML (1991) CANDIDATES FOR THE MECHANOSENSORY SYSTEM IN BONE. Journal of Biomechanical Engineering-Transactions of the Asme 113 (2): 191-197. https://doi.org/10.1115/1.2891234

[21] Patel K, Brandstetter K (2016) Solid Implants in Facial Plastic Surgery: Potential Complications and How to Prevent Them. Facial Plastic Surgery 32 (5): 520-531. https://doi.org/10.1055/s-0036-1586497

[22] Lee T-Y, Chung H-Y, Dhong E-S, et al (2019) Paranasal Augmentation Using Multi-Folded Expanded Polytetrafluorethylene (ePTFE) in the East Asian Nose. Aesthetic Surgery Journal 39 (12): 1319-1328. https://doi.org/10.1093/asj/sjz103

[23] Nocini PF, Boccieri A, Bertossi D (2009) Gridplan Midfacial Analysis for Alloplastic Implants at the Time of Jaw Surgery. Plastic and Reconstructive Surgery 123 (2): 670-679. https://doi.org/10.1097/PRS.0b013e318196b958

[24] Wang L, Kang JF, Sun CN, et al (2017) Mapping porous microstructures to yield desired mechanical properties for application in 3D printed bone scaffolds and orthopaedic implants. Materials & Design 133: 62-68. https://doi.org/10.1016/j.matdes.2017.07.021

[25] Sun CN, Wang L, Kang JF, et al (2018) Biomechanical Optimization of Elastic Modulus Distribution in Porous Femoral Stem for Artificial Hip Joints. Journal of Bionic Engineering 15 (4): 693-702. https://doi.org/10.1007/s42235-018-0057-1

[26] Kang J, Zhang J, Zheng J, et al (2021) 3D-printed PEEK implant for mandibular defects repair-a new method. Journal of the Mechanical Behavior of Biomedical Materials 116: 104335. https://doi.org/10.1016/j.jmbbm.2021.104335

[27] Wang D, Qu A, Zhou H, et al (2016) BIOMECHANICAL ANALYSIS OF THE APPLICATION OF ZYGOMA IMPLANTS FOR PROSTHESIS IN UNILATERAL MAXILLARY DEFECT. Journal of Mechanics in Medicine and Biology 16 (8): 1640030.

Preprint of Bio Design and Manufacturing (unedited)

https://doi.org/10.1142/s0219519416400303

[28] Miyamoto S, Ujigawa K, Kizu Y, et al (2010) Biomechanical three-dimensional finite-element analysis of maxillary prostheses with implants. Design of number and position of implants for maxillary prostheses after hemimaxillectomy. International Journal of Oral and Maxillofacial Surgery 39 (11): 1120-1126. https://doi.org/10.1016/j.ijom.2010.06.011

[29] Zhang J, Li D, Liu Y, et al (2022) Application of Patient-Specific PEEK Implant for Aesthetic Considerations in Paranasal Augmentation. Journal of Craniofacial Surgery 33 (8): E877-E880. https://doi.org/10.1097/scs.0000000000008824

[30] Monje A, Ravida A, Wang H-L, et al (2019) Relationship Between Primary/Mechanical and Secondary/Biological Implant Stability. International Journal of Oral & Maxillofacial Implants 34: S7-+: Pmid 31116830. https://doi.org/10.11607/jomi.19suppl.g1

[31] Sharma N, Welker D, Aghlmandi S, et al (2021) A Multi-Criteria Assessment Strategy for 3D Printed Porous Polyetheretherketone (PEEK) Patient-Specific Implants for Orbital Wall Reconstruction. Journal of Clinical Medicine 10 (16): 3563. https://doi.org/10.3390/jcm10163563

[32] Torstrick FB, Safranski DL, Burkus JK, et al (2017) Getting PEEK to Stick to Bone: The Development of Porous PEEK for Interbody Fusion Devices. Techniques in orthopaedics (Rockville, Md) 32 (3): 158-166. https://doi.org/10.1097/bto.0000000000000242

[33] Moiduddin K, Mian SH, Elseufy SM, et al (2023) Polyether-Ether-Ketone (PEEK) and Its 3D-Printed Quantitate Assessment in Cranial Reconstruction. Journal of Functional Biomaterials 14(8): 429. https://doi.org/10.3390/jfb14080429

[34] Belwanshi M, Jayaswal P, Aherwar A (2022) Mechanical behaviour investigation of PEEK coated titanium alloys for hip arthroplasty using finite element analysis[C]. Mohali, INDIA, 56(5): 2808-2817. https://doi.org/10.1016/j.matpr.2021.10.112

[35] Kang JF, Wang L, Yang CC, et al (2018) Custom design and biomechanical analysis of 3D-printed PEEK rib prostheses. Biomechanics and Modeling in Mechanobiology 17 (4): 1083-1092. https://doi.org/10.1007/s10237-018-1015-x

[36] Bruzauskaite I, Bironaite D, Bagdonas E, et al (2016) Scaffolds and cells for tissue regeneration: different scaffold pore sizes-different cell effects. Cytotechnology 68 (3): 355-369. https://doi.org/10.1007/s10616-015-9895-4

[37] Taniguchi N, Fujibayashi S, Takemoto M, et al (2016) Effect of pore size on bone ingrowth into porous titanium implants fabricated by additive manufacturing: An in vivo experiment. Materials Science and Engineering: C 59: 690-701. https://doi.org/https://doi.org/10.1016/j.msec.2015.10.069

[38] Fukuda A, Takemoto M, Saito T, et al (2011) Osteoinduction of porous Ti implants with a channel structure fabricated by selective laser melting. Acta Biomaterialia 7 (5): 2327-2336. https://doi.org/10.1016/j.actbio.2011.01.037

[39] Bai F, Zhang JK, Wang Z, et al (2011) The effect of pore size on tissue ingrowth and neovascularization in porous bioceramics of controlled architecture in vivo. Biomedical Materials 6 (1): 015007. https://doi.org/10.1088/1748-6041/6/1/015007

[40] Zadpoor AA (2015) Bone tissue regeneration: the role of scaffold geometry. Biomaterials Science 3 (2): 231-245. https://doi.org/10.1039/c4bm00291a

[41] Nune KC, Kumar A, Misra RDK, et al (2017) Functional response of osteoblasts in functionally gradient titanium alloy mesh arrays processed by 3D additive manufacturing. Colloids and

Preprint of Bio Design and Manufacturing (unedited)

Surfaces B-Biointerfaces 150: 78-88. https://doi.org/10.1016/j.colsurfb.2016.09.050

[42] Zheng JB, Zhao HY, Ouyang ZC, et al (2022) Additively-manufactured PEEK/HA porous scaffolds with excellent osteogenesis for bone tissue repairing. Composites Part B-Engineering 232: 109508. https://doi.org/10.1016/j.compositesb.2021.109508

[43] Gómez S, Vlad MD, López J, et al (2016) Design and properties of 3D scaffolds for bone tissue engineering. Acta Biomaterialia 42: 341-350. https://doi.org/https://doi.org/10.1016/j.actbio.2016.06.032

[44] Lu SW, Zhang BN, Niu JY, et al (2024) Effect of fiber content on mechanical properties of carbon fiber-reinforced polyether-ether-ketone composites prepared using screw extrusion-based online mixing 3D printing. Additive Manufacturing 80: 103976. https://doi.org/10.1016/j.addma.2024.103976

Preprint of Bio-Design and Manufacturing (unedited)